UNCERTAINTY ANALYSIS OF AIRBORNE LIDAR DATA ACQUISITION IN GRAIN FIELD

János Tamás *, Erika Buday-Bódi, Dávid Pásztor, Attila Nagy, Zsolt Zoltán Fehér

Institute of Water and Environmental Management, Faculty of Agricultural and Food Sciences and Environmental Management, University of Debrecen, Hungary * Correspondence: tamas@agr.unideb.hu

DOI: 10.66538/DH.2025.1.1.52

Abstract

In this paper, our aim to evaluate the measurement possibilities that lidar sensor provide for new opportunities in precision agriculture. Applied Aircraft DJI Matrice 300 was with the Zenmuse L1, where the Livox Avia uses a 905nm near infrared wavelength laser to measure distances and implemented a high-accuracy IMU, and a camera with a 1-inch CMOS on a 3-axis stabilized gimbal. When used with Matrice 300 RTK and DJI Terra, the L1 forms a complete solution that gives for users a real-time 3D data, efficiently capturing the details of complex structures and delivering highly accurate reconstructed field models. The relative altitude was set to 30 m, flight speed to 2 m/s, gimbal pitch to -90°, and each straight segment of the flight route was less than 1000 m. The originally urban indices are also useful results in the topological evaluation of agricultural biomass during precision agricultural technology developments. In LIDAR scanning, the vegetation target has a complex spatial structure, so it is important that the laser point cloud data should be representative of the plant morphology in field condition. This structure is typical for each plant and its developmental stages. In the case of our target was oats (Avena sativa L.). The flight altitude increases, most of the error source increase as well (except for those associated with GPS) however, if increasing the flight altitude improves the size of the surveyed area. When planning a flight mission, the accuracy and precision parameters to be achieved based on the survey must be precisely optimized to ensure that the vegetation LIDAR metric is processed to provide.

Keywords: agriculture, UAV, LIDAR, photogrammetry.

1. Introduction

Combining agricultural robots (agribots) with other advanced technologies primarily in the field data real time collection of IoT sensors and artificial intelligence related to data cloud processing promises significant progress for various agricultural technological developments [1,2] primarily for the development of autonomous and intelligent vehicles and autonomous agricultural robots. The use of drones in agriculture is also a particularly promising area for future developments both applied areas to survey agroecosystems [3] and carry out precision operative tasks. The yearly expansion in the overall production of cereals & the adoption of smart farming techniques for generating maximum output would also drive the application of drones in the coming years [4]. The potential for using drones on farms by 2050 seems truly vast. It covers everything from imaging and applying products with precision to transporting supplies around. And it extends to carrying out farm tasks that nobody has quite pictured yet. [5,6].

In the case of survey drones, with the increasing play load capacity are more effectively used, because the miniaturized sensors capable to carry out increasingly complex remote sensing operations and share more data sources [7].

Study published by Tamás et al. (2015) has demonstrated that species-level identification and mapping of weeds can be performed based on ground laser scanned laser point cloud segmentation [8].

Manas Wakchaure at al. (2023) [9] summarized experiences a 60-year long period overview of 150 publications based on systematic study of AI techniques in the field of agriculture and concluded that one of the important AI areas of future research

will be the investigation of the application of intelligent autonomous systems with applied AI hybrid algorithm in agriculture. More study was published when an unmanned aerial vehicle (UAV) was used to collect many images from canopy in an early stage of infection for the generation of a training dataset for which it is necessary to employ more complex procedures, such as machine learning (ML) or partial least squares regressions (PLSR) algorithms [10, 11, 12]. Although there are many sensor examples of the use of different electromagnetic spectra in precision agriculture [13, 14] there is much less information on the high accuracy description of the three-dimensional agricultural environment such as canopy or tree structures that many crop production applications would require [15]. The cameras with high ground resolution mounted on UAV drones, can collect stereo graphic three-dimensional images, and based on photogrammetric postprocessing produce a three-dimensional digital surface model of the scanned agricultural area [16, 17]. The disadvantage of this photogrammetric method is that there is no penetration into the biomass deeper layers for example, leaves overlap each other within the foliage, the data set will not be able to describe the interior topological structure of the vegetation. This disadvantage can be overcome by another survey method which is conducted by laser scanning because here the laser light beam is used with a high depth penetration [18].

In this paper, our aim is to evaluate the measurement possibilities that lidar sensors provide for new opportunities in precision agriculture. Our results will be validated by field agronomic measurements.

2. Materials and Methods

The experimental setup was developed by Kutassy et al where goal was to evaluate spectral remote sensed UAV data sources in the foliar fertilization treatment experiments [19]. The measurements were taken in a small plot (1.5 × 7 m = 10.5 m^2) experiment, with three independent repetitions, where six winter oat (*Avena sativa* L.) genotypes that were evaluated on n=72 plots (Figure 1.).

Figure 1. 3D point clouds of the experimental area indicated by green strips

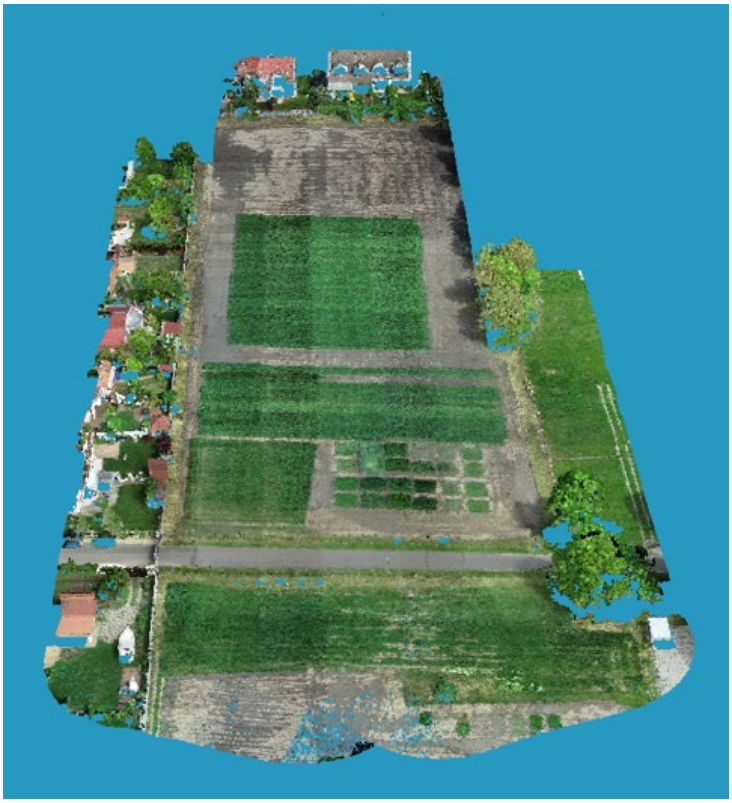

The corner points of each experimental parcel polygon boundaries and ground control points (GCP) coordinates were surveyed with Stonex S9i RTK GPS using the Stop&Go technique. Field survey information, thereafter, were processed in the ESRI ArcGIS

Pro 3.8 ver. software environment, where each parcel was interpreted as a rectangular. These polygons individually provided the spatial extent of the other attributes. Thereby the spatial connection of the versatile measured and calculated parameter set is given in the joint attributive parameter table.

The Normalized Difference Vegetation Index NDVI values were observed using on-field GreenSeeker Trimble (Sunnyvale, California, USA) [20] hand-held spot crop sensor and drone-based imagery. A DJI Phantom 4 Pro V2 UAV drone equipped with Sentera Double 4K TrueNDVI and TrueNDRE sensors [21] was used to record remotely sensed $NDVI_{UAV}$ and $NDRE_{UAV}$ spectral index images. The orthorectified photos were analyzed in DJI Terra (DJI) [22] and ENVI 5.3 (Hexagon) software. Then by the ArcGis Pro software, the raster was recalculated using the formula, and zone statistics were used to determine the mean and standard deviation values on each plot. Total chlorophyll content assessment was carried out on leaf samples taken on 24 June (BBCH 77). Leaf samples were preserved and prepared for analysis according to the findings of Szabó et al. [23]. Grain samples were taken from each plot to determine the grain moisture content and weight. The agronomic data of experiments was published earlier [24], but in the frame of this study we focus on computing aspects.

3. Results

LiDAR survey technology is the key methodological area of this publication, so the measurement methods used here are discussed in more detail below. LiDAR stands for Light Detection and Ranging, a technology that measures distances (or ranges) based on the time between transmitting and receiving laser signals. During the LIDAR flying campaign the experimental sites were scanned four times, 10. May 24. May (BBCH52), 07. June (BBCH65), 21. June (BBCH77). These dates were close to the spectral UAV measurements and fell within the time interval of the most important plant morphological changes for crop production from beginning of heading flowering to late milk of grain. At the beginning of the process, the plant has already reached almost its top height, the whole photosynthetically active canopy including the most important flag leaf has developed, but at the end of the process, the shaded leaves close to the soil surface have not yet started to senesce and dry. Applied Aircraft DJI Matrice 300 was with the Zenmuse L1, where the Livox Avia uses a 905nm near infrared wavelength laser to measure distances and implemented a high-accuracy IMU, and a camera with a 1-inch CMOS on a 3-axis stabilized gimbal. When used with Matrice 300 RTK and DJI Terra, the L1 forms a complete solution that gives users real-time 3D data, efficiently capturing the details of complex structures and delivering highly accurate reconstructed field models.

The relative altitude was set to 30 m, flight speed to 2 m/s, gimbal pitch to -90°, and each straight segment of the flight route was less than 1000 m.

Measured in an environment of 20-25℃ with a target (80% reflectivity) 100 meters away. Pitch/Roll Accuracy（RMS 1σ）Real-time: 0.05°, Post-processing: 0.025°. Although in farm condition the result may vary under different test conditions during this flight campaigns, we carried out the survey under optimal weather conditions wind speed < 1 m s-1, Rh% < 70%, cloud cover < 10%, solar angle close to zenith, visual distance min. 300 m,). In the case of LIDAR surveys, when the target a non-solid surface, e.g. canopy, it is especially important to measure without any wind, because the movement of the leaves of the plants can produce significant geometrical measurement noise.

The applied DJI L1 sensor parametrized with Field of View (FoV) repetitive scanning pattern: 70.4° (horizontal) × 4.5° (vertical). IMU Update Frequency was 200 Hz, where Yaw Accuracy（RMS 1σ）Real-time: 0.3°, Post-processing: 0.15°. The L1 provides three scanning frequencies: one/two returns: 80K/s, 160K/s, and 240K/s; three returns: 80K/s, 240K/s.

Auxiliary positioning resolution of RGB vision sensor mapping camera 1280×960, FOV 95°, 20Mpixel, Data storage microSD with sequential writing speed 50 MB/s. Post-processing software was DJI Terra that use point cloud data format. The L1 camera requires precision GPS data in either RTK or PPK mode. In this case Zenmuse L1 LIDAR geoprocessing was carried out in PPK mode. Post-processed kinematic (PPK) is a method of using Global Navigation Satellite System (GNSS) data to accurately determine the position and trajectory of a rover/drone. PPK involves collecting raw GNSS data from a drone, along with information about the position and trajectory of nearby reference stations, and then processing the data after the fact to improve the accuracy of the

position and trajectory information [25]. Longer Post-Processing Time: PPK requires post-processing of data, which can take time and delay the delivery of the final product. The distance between the TRIMBLE geobase station and the rover was less than 1 km during the campaign.

LIDAR airborne flying campaigns output data was sequential binary LASer - LAS 1.4. versions refer to the predefined classification schemes defined by ASPRS for each data category. LAS is an industry format created and maintained by the American Society for Photogrammetry and Remote Sensing (ASPRS) [26]. The LAS lidar point attributes are maintained for each laser pulse of a LAS file: x, y, z location information, GPS time stamp, intensity, return number, number of returns, point classification values, scan angle, additional RGB values, scan direction, edge of flight line, user data, point source ID, and waveform information as a metadata. The standard LiDAR equation relates the power of transmitted *(P_t)* and received (P_r) signals, and can be expressed as eq.1 [27]:

$$P_r(t) = \frac{D^2}{4\pi\lambda^2}\int_0^H \frac{\eta_{SYS}\eta_{atm}}{R^4} P_t\left(t - \frac{2R}{v_g}\right)\sigma(R)dR \qquad \text{eq. 1}$$

where t is the time; *D* is the aperture diameter of the receiver optics; P_r is the power of received signal; P_t is the power of transmitted signal; λ is the wavelength; *H* is the flying height; *R* is the distance from the system to the target; η_{sys} and η_{atm} are the system and atmospheric transmission factors, respectively; v_g is the group velocity of the laser pulse; and $\sigma(R)dR$ is the apparent effective differential cross section.

The most useful characteristic of LiDAR might be that the laser energy can penetrate through canopy gaps and measure canopy structural and terrain elevation along the direction of laser rays. In LIDAR scanning, the vegetation target has a complex spatial structure, so it is important that the laser point cloud data should be representative of the plant morphology in field condition [27]. This structure is typical for each plant and its developmental stages. In the case of our target was oats (Avena sativa L.), so we briefly describe the main structural properties. Oats are an annual crop with tall and short stature depending on the presence of dwarfing alleles. Each plant produces about five stems depending on the growing season and each stem produces about five to six leaves on dwarf stature plants and eight to ten leaves on tall plants. Each stem or culm produces a terminal panicle where the seeds develop. Plant height will vary with growing season and the presence or absence of dwarfing alleles. Varieties with dwarfing alleles will vary in height between 45 and 70 cm [28]. The major developmental stages of plant growth are germination, leaf production, tiller production, stem elongation, panicle development and emergence, anthesis, grain filling, and ripening. Unlike wheat, barley, and rye, oats form a panicle composed of branches with the seed produced at the tip. Flowering or anthesis occurs when pollen is shed on the feathery stigmas enclosed by the lemma and palea with outer tissues called glumes. This stage occurs when the panicle has fully emerged from the flag leaf in tall varieties but may occur while the head is still contained in the flag leaf for dwarf varieties. Grain size and weight increase as sugars are converted to starch [29]. As the seed matures, the plant begins to lose moisture and senesces. The mature oat grain consists of a groat, or caryopsis tightly covered by a hull or husk previously the lemma and palea. The hull represents 30-40% of the total grain weight. It is comprised of cellulose, hemicellulose, and lignin. Compared to other cereals, the oat groat is slender and covered with hairs or trichomes under the hull [30].

The most frequently calculated urban LiDAR metrics are follows: Minimum; Maximum; Range; Arithmetic Mean (μ) ; Standard Deviation (σ); Variance (σ^2); Coefficient of Variation: *(σ/μ)*100;* Percentiles: *5th, 10th, 25th, 50th, 75th*, and *95th* percentile values (x); Median; Dominate Mode: Value of the dominate mode in a kernel density estimate (*x*); Skewness; Kurtosis; Interquartile range: *75th* percentile (*x*) – *25th* percentile (*x*); Number of Modes: Number of modes from a kernel density estimate (x); Difference between Min and Max Mode: (maximum mode – minimum mode) from a kernel density estimate (x); Percent of returns that are first, second, third; Texture: $\sigma(n_i|>$ height(0) and <= height(1)|). These originally urban indices are also useful tools in the topological evaluation of agricultural biomass during precision agricultural technology developments (Figure 2,3).

Figure 2. Plot mean heights calculated based on LIDAR data (C-control, Si -Silica, S-Sulfur)

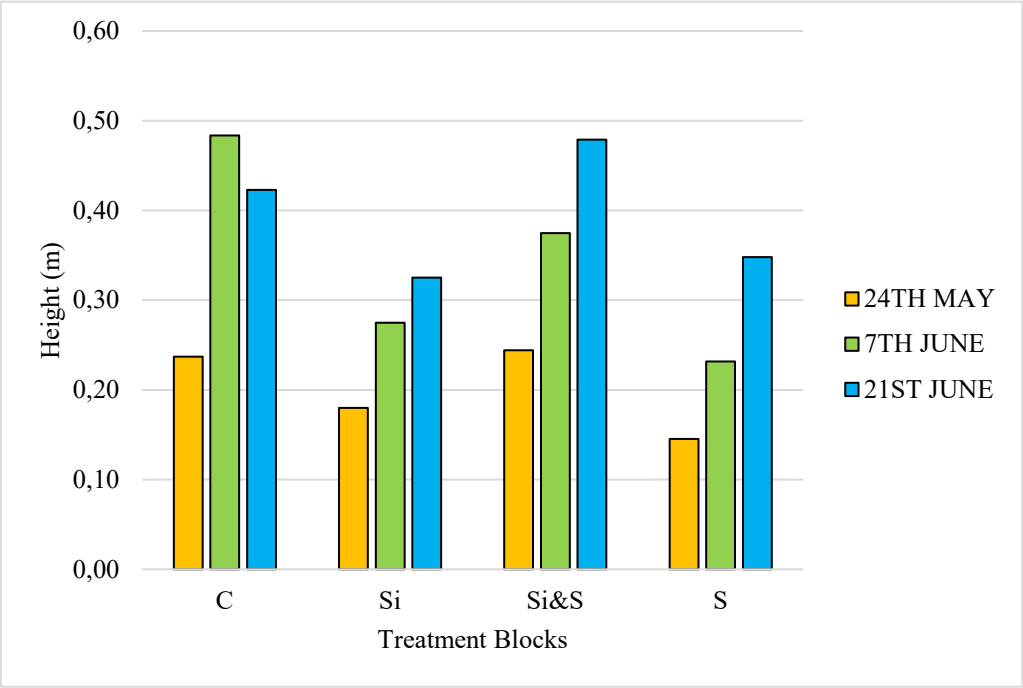

Figure 3. LiDAR point dense map before filtering

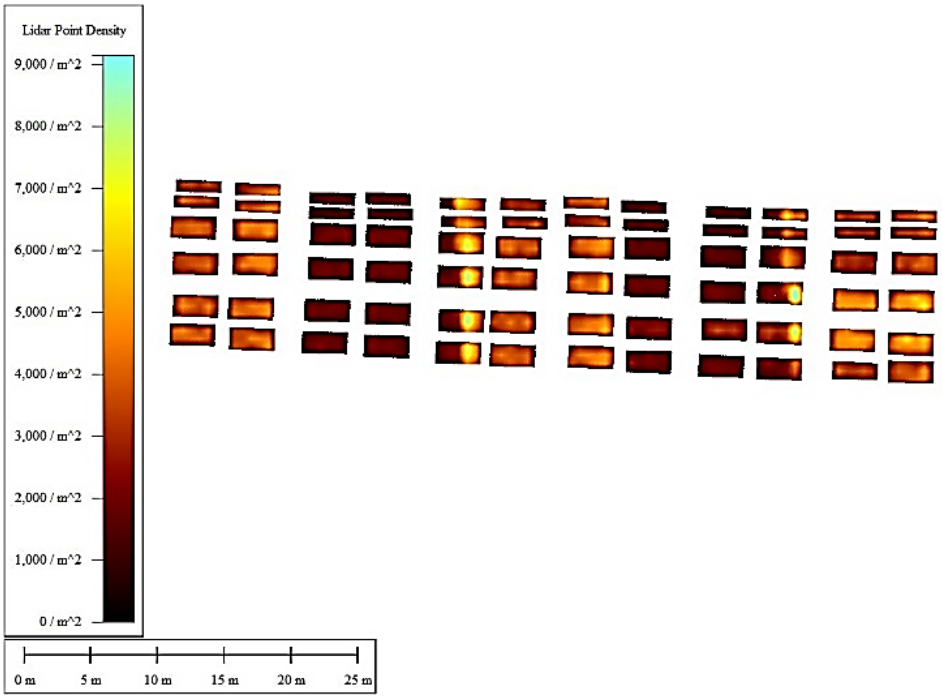

4. Discussion

Oats have played a significant role in farming systems from domestication to present due to the versatile uses of the grain and plant. Oats currently rank sixth in world production of cereals after maize, rice, wheat, barley, and sorghum. World oat production was like millet and exceeded rye, and triticale. Oats are a versatile crop used as grain and fodder for animal feed, human foods, industrial products, cosmetics, and pharmaceuticals. If the condition of the oats could be measured in the field, as it is intended to be used, this would be very valuable information, but this requires the development of an appropriate measurement method.

Although lidar can provide precise and accurate measurements, there are so many components (LiDAR, vertical/horizontal GPS, horizontal IMU, Rectification) that go into getting those measurements that if even just one of those is inaccurate, it will compound decreasing the overall accuracy of the dataset [31]. The flight altitude increases, most of the error source increase as well (except for those associated with GPS) however, if increasing the flight altitude improves the size of the surveyed area. When planning a flight mission, the accuracy and precision parameters to be achieved based on the survey must be precisely optimized to ensure that the vegetation LIDAR metric is processed to provide. To calculate LiDAR accuracy the standard deviation (σ^2) and root mean square error (RMSE) statistical comparison between surveyed flat bare concrete surface (slopes lower than 0.01%) points and measured laser points, were applied [32]. The data processing process is summarized in Figure 4.

Figure 4. Flowchart of LIDAR point data processing

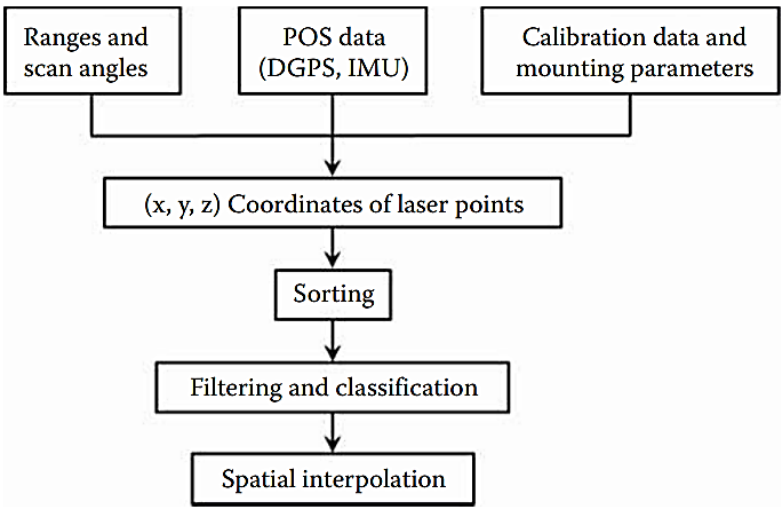

Based on automatic point cloud object segmentation of ASPRS Standard Classes for Point Data Record, 3 vegetation types can be distinguished: high, medium and low vegetation classes but a user should carefully check the documents provided by the LiDAR vendor to understand how points have been classified specifically. Biomass is a typical soft object, where multipath propagation errors are orders of magnitude more common than hard objects, for example, in the case of flat road surfaces, building roofs. Thus, the number of unsigned points numbers is relatively increased during automatic classification.

Since these classes are not suitable for a more accurate assessment of agricultural vegetation, it is recommended to introduce new classes which are presented on the vertical structure oat vegetation.

Figure 5. The most important agronomic vertical zones of the lasers scanned oat.

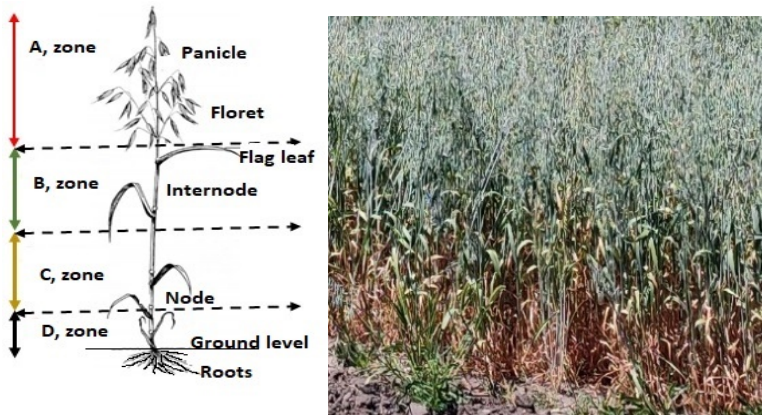

Based on the 5. Figure, during the classification of the LiDAR point cloud, vertical zones of cereal vegetation should be classified according to 4 zones from the point of view of agronomic use.

In the case of photogrammetry quality assessment, an artificial, perfectly smooth (slope 0,001%) surface of a few square meters with a known slope is usually assessed in practice, which showed a scanning inclination angle like flight bands, preferably close to nadir ±5%. In this case, we used a smoothed concrete surface, which was located 15 m from the test site and was part of the aerial data collection.

A reference point data with sample number n=1035 was selected by hand digitization from a brick-based space on a 0% slope. Ground control points were also measured on the concrete surface with a pair of STONEX RTK meters based on RTK GPS measurement mode Thus, the absolute and WGS84 relative x-y-z coordinates were available. Basic statistical data summarized based on the set of points measured on the reference surface after photogrammetry processing (Table 1).

Table 1. The vertical and horizontal point distances on the reference surface.

Elevation	Distance 2D (mm)	Distance 3D (mm)
mean	2,721	13,868
median	2,723	13,89
variance	0,23	0,65

Based on the above, the survey was highly accurate. Here, too, practical experience was confirmed by the fact that horizontal accuracy was better than vertical, but both dimensions are suitable for topographic assessment of plant topology. It was also expected that the first returnees from the uncovered concrete surface occurred in an order of magnitude higher numbers than in the case of cereal crops, where this was caused by its complex topology.

5. Conclusions

Compared with multispectral, hyperspectral, thermal UAV remote sensing LiDAR remote sensing is a relatively new field of precision agriculture. In an optical UAV image of the passive sensor, the value of each pixel is dominated by the spectral reflectance of the object surface, and there is no information on the soil or topography if the ground surface is covered by dense canopy.

The application of lidar technology in crop production provides many new potential opportunities for agriculture. One of the determining criteria for plant development is to ensure that all individuals have access to the necessary water, nutrients and light during development. To ensure this, it is necessary to create an optimal spatial structure of vegetation with the best biomass space filling. The new point cloud 3D based spatial data model allows precision agricultural machinery to be redesigned to better adapt to changes in plant topology.

To improve consistency of the LiDAR project additionally, visualization software Q/A should be used to check the accuracy of point zone classification and fitting to phenology of vegetation.

The LIDAR adaptive indicators must be selected for suitable, flexible applied technology in different phenological and environmental conditions. The homogeneous management zones of the agricultural fields must be segmented based on geostatistical analysis of the LIDAR indicators. It is necessary to plan the spatially differentiated agrotechnological operations applicable in zones. As a result of these LIDAR processes, Agriculture 5.0 will reach a new level of autonomous automated robotization.

6. Acknowledgments

The research presented in the article was carried out within the framework of the Széchényi Plan Plus program with the support of the RRF 2.3.1 21 2022 00008 project.

References

1. Ahmad, L., and Nabi, F. AGRICULTURE 5.0 . 2021. CRC Press, Taylor & Francis Group, LLC. p.219. ISBN: 978-0-367-64610-3
2. Choudhury, A., Biswas, A., Prateek, M., and Chakrabarti, A. (eds)Agricultural Informatics Automation Using the IoT and Machine Learning (2021) Publ. John Wiley & Sons, p. 271. ISBN 978-1-119-76884-5
3. Trappey, A.J.C., Lin, G.-B., Chen, H.-K., and Chen, M.-C., A comprehensive analysis of global patent landscape for recent R&D in agricultural drone technologies, World Patent Information, Volume 74, 2023, 102216, ISSN 0172-2190,
4. Europe Agriculture Drones Market Research Report: Forecast (2023-2028). Jan 2023 Report Code ET55029 Pages 182. Available online: https://www.marknteladvisors.com/research-library/europe-agriculture-drones-market.html
5. Rejeb, A., Abdollahi, A., Rejeb, K., and Treiblmaier, H., Drones in agriculture: A review and bibliometric analysis, Computers and Electronics in Agriculture, Volume 198, 2022, 107017, ISSN 0168-1699,
6. Edulakanti, S.R., and Ganguly, S., Review article: The emerging drone technology and the advancement of the Indian drone business industry, The Journal of High Technology Management Research, Volume 34, Issue 2, 2023,100464, ISSN 1047-8310,
7. Caruso, G., Palai, G., Tozzini, L., D'Onofrio, C., and Gucci, R., The role of LAI and leaf chlorophyll on NDVI estimated by UAV in grapevine canopies, Scientia Horticulturae, Volume 322, 2023, 112398, ISSN 0304-4238, https://doi.org/10.1016/j.scienta.2023.112398.
8. Riczu, P.; Nagy, A.; Tamás, J.; Lehoczky, É. Precision weed detection using terrestrial laser scanning techniques. Commun. Soil Sci. Plant Anal. 2015, 46, 309–316.
9. Manas Wakchaure, B.K. Patle, A.K. Mahindrakar, Application of AI techniques and robotics in agriculture: A review, Artificial Intelligence in the Life Sciences, Volume 3, 2023, 100057, ISSN 2667-3185,
10. Wu, B., Liang, A., Zhang, H., Zhu, T., Zou, Z., Yang, D., Tang, W., Li, J., and Su, J., Application of conventional UAV-based high-throughput object detection to the early diagnosis of pine wilt disease by deep learning, Forest Ecology and Management, Volume 486, 2021, 118986, ISSN 0378-1127, https://doi.org/10.1016/j.foreco.2021.118986.
11. Lan, Y., Huang, Z., Deng, X., Zhu, Z., Huang, H., Zheng, Z., Lian, B., Zeng, G., and Tong, Z., Comparison of machine learning methods for citrus greening detection on UAV multispectral images, Computers and Electronics in Agriculture, Volume 171, 2020, 105234, ISSN 0168-1699, https://doi.org/10.1016/j.compag.2020.105234.
12. Wang, T., Chen, B., Zhang, Z., Li, H., and Zhang, M., Applications of machine vision in agricultural robot navigation: A review, Computers and Electronics in Agriculture, Volume 198, 2022, 107085, ISSN 0168-1699, https://doi.org/10.1016/j.compag.2022.107085.
13. Kiss, N. Éva.; Tamás, J.; Szőllősi, N; Gorliczay, E; Nagy, A. Assessment of Composted Pelletized Poultry Litter as an Alternative to Chemical Fertilizers Based on the Environmental Impact of Their Production. AGRICULTURE-BASEL 11: 11 Paper: 1130 (2021)
14. Mézes, L.; Nagy, A.; Gálya, B.; Tamás, J, Poultry feather wastes recycling possibility as soil nutrient. EURASIAN JOURNAL OF SOIL SCIENCE 4: 4 pp. 244-252. , 9 p. (2015)
15. K. R. Krishna Agricultural drones, A Peaceful Pursuit. 2018. Publ. Apple Academic Press, USA. p. 413. ISBN: 978-1-77188-595-9
16. Neugerg, F.; Kaiseer, A.; Schmidt, J.; Becht, M.; Haas, F. Quantification, Analysis and Modelling of Soil Erosion on Steep Slopes Using LiDAR and UAV Photographs. Proceedings of a Symposium on Sediment Dynamics. New Orleans, Louisiana, USA, 2015, IAHS Publication No. 367: 51–76.
17. Kőmíves T, Béres I, Reisinger P, Lehoczky É, Berke J, Tamás J, Páldy A, Csornai G, Nádor G, Kardeván P, Mikulás J, Gólya G, Molnár J: A parlagfű elleni integrált védekezés új stratégiai programja, MAGYAR GYOMKUTATÁS ÉS TECHNOLÓGIA 7: (1) pp. 5-50.
18. Miguel F. Acevedo Real-Time Environmental Monitoring. 2nd edition. p. 425. 2024. Publ. CRC Press USA ISBN: 978-1-032-54571-4. DOI: 10.1201/9781003425496
19. Kutasy, E.; Buday-Bódi, E.; Virág, I.C.; Forgács, F.; Melash, A.A.; Zsombik, L.; Nagy, A.; Csajbók, J. Mitigating the Negative Effect of Drought Stress in Oat (Avena sativa L.) with Silicon and Sulphur Foliar Fertilization. Plants 2022, 11, 30. https://doi.org/10.3390/plants11010030.
20. Rouse, W.J.; Haas, R.H.; Schell, J.A.; Deering, D.W. Monitoring Vegetation Systems in the Great Plains with ERTS. In Proceedings of the Third ERTS Symposium, Washington, DC, USA, 10–14 December 1973; pp. 309–317.
21. Sentera. 2021. Available online: https://support.sentera.com/portal/en/kb/sentera (accessed on).

22. DJI Terra Download Center. China, https://www.dji.com/hu/dji-terra/info (accessed on).
23. Szabó, A.; Tamás, J.; Nagy, A. The influence of hail net on the water balance and leaf pigment content of apple orchards. Sci. Hortic. 2021, 283, 110112.
24. Csajbók, J.; Buday-Bódi, E.; Nagy, A.; Fehér, Z.Z.; Tamás, A.; Virág, I.C.; Bojtor, C.; Forgács, F.; Vad, A.M.; Kutasy, E. Multispectral Analysis of Small Plots Based on Field and Remote Sensing Surveys—A Comparative Evaluation. Sustainability 2022, 14, 3339. https://doi.org/10.3390/su14063339
25. Complete PPK Workflow for DJI Enterprise Drones DJI Learning Center. Available online: https://enterprise-insights.dji.com/blog/ppk-post-processed-kinematics-workflow
26. LAS Specification v.1.4-R15 American Society for Photogrammetry&Remote Sensing. 2011. Publ. ASPRS USA p. 47. https://www.asprs.org
27. McManamon, P. LiDAR technologies and systems. Publ. SPIE Press USA p. 523. ISBN 9781510625402
28. Bonnett O.T. (1961) Morphology and Development. In: Coffman, F.A. (ed.) Oats and Oat Improvement, vol. 8, pp. 4174. Madison, Wisconsin: American Society of Agronomy.
29. Yong-Bi Fu Oat evolution revealed in the maternal lineages of 25 Avena species. Journal: Scientific Reports, 2018, Volume 8, Number 1. DOI: 10.1038/s41598-018-22478-4
30. Ladizinsky, G. (2012). Oat Morphology and Taxonomy. In: Studies in Oat Evolution. SpringerBriefs in Agriculture. Springer, Berlin, Heidelberg. https://doi.org/10.1007/978-3-642-30547-4_1
31. Stallings, C. Understanding the Accuracies of the DJI Zenmuse L1. Publ. March 28, 2023. BAAM TECH https://baam.tech/dji-zenmuse-l1-geospatial-accuracies/ (accessed on)
32. Evans, J.S., Hudak, A.T., Faux, R., and Smith, A.M.S., 2009. Discrete return lidar in natural resources: Recommendations for project planning, data processing, and deliverables. Remote Sensing, 1: 776–794.